NUMERICAL SIMULATION OF RADIAL AND AXIAL EVOLUTION OF REDUCED ELECTRIC FIELD ON THE CONVERSION OF NITROGEN OXIDES

SIMULACIÓN NUMÉRICA DE LA EVOLUCIÓN RADIAL Y AXIAL DEL CAMPO ELÉCTRICO REDUCIDO EN LA CONVERSIÓN DE ÓXIDOS DE NITRÓGENO

A. K. Ferouani[a,b†], M. Lemerni[b], S. Belhour[c], S. Askri[d]

a) Ecole Supérieure en Sciences Appliquées, Tlemcen, 13000, Algeria; ferouani_karim@yahoo.fr†
b) L.P.T Laboratory, University A. Belkaid of Tlemcen, 13000, Algeria.
c) L.P.M.P.S, Department of Physics, Faculty of Exact Sciences, University of Freres Mentouri, Constantine 1, 25000 , Algeria.
d) L.E.V.R.E.S Laboratory, University of El Oued, 39000, Algeria.
† corresponding author

Recibido 01/9/2020; Aceptado 05/10/2020

In this paper, we propose to numerically simulate the spatial-temporal (axial and radial) evolution of the density of certain nitrogen oxides present in the gaseous mixture: 74 % N_2, 10 % O_2, 8 % H_2O and 8 % CO_2 which is subject to a negative corona discharge at room temperature and atmospheric pressure. We study the influence of the reduced electric field E/n (E electric field, n the density) on the chemical kinetics of this mixture. The gas chemistry takes into account 18 species such as: the radicals N, O, H, OH, the ground state molecules N_2, O_2, H_2O, CO_2, O_3, H_2, HNO_3, the nitrogen oxides NO, N_2O, NO_2, NO_3, N_2O_5, metastable species $N(^2D)$ and the electrons e^-, reacting with one another 80 selected chemical reactions. The purpose of this simulation is to complete these studies by analyzing different plasma species under three selected values of reduced electric fields: 100, 200 and 300 Td. The results obtained show an evolution closely related to the reduced electric field.

En este trabajo, proponemos simular numéricamente la evolución temporal (axial y radial) de la densidad de determinados óxidos de nitrógeno presentes en la mezcla gaseosa: 74 % N_2, 10 % O_2, 8 % H_2O y 8 % CO_2 sujeta a una descarga corona negativa a temperatura ambiente y presión atmosférica. Estudiamos la influencia del campo eléctrico reducido E/n (E campo eléctrico, n la densidad) sobre la cinética química de esta mezcla. En la química del gas se tienen en cuenta 18 especies como: los radicales N, O, H, OH, las moléculas del estado fundamental N_2, O_2, H_2O, CO_2, O_3, H_2, HNO_3, el óxido de nitrógeno NO, N_2O, NO_2, NO_3, N_2O_5, especies metastable $N(^2D)$ y los electrones e^-, que reaccionan entre sí mediante 80 reacciones químicas seleccionadas. El propósito de esta simulación es completar estos estudios analizando diferentes especies plasmáticas con tres valores seleccionados de campos eléctricos reducidos: 100, 200 y 300 Td. Los resultados obtenidos muestran una evolución estrechamente relacionada con el campo eléctrico reducido.

PACS: Corona discharges (descargas de corona), 52.80.Hc; plasma kinetic equations (ecuaciones cinéticas de plasma), 52.25.Dg; plasma simulation (simulación de plasma), 52.65.-y.

I. INTRODUCTION

Nowadays, gas discharge plasmas and their applications in physics, chemistry, biology, and environmental programs are being widely studied. They can be used for reforming the poisonous pollutants, such as NO_x, SO_x, CO_x. These studies are based on the numerical equations for the reduction of NO_x gases in reactors [1,2].

Plasmas are able to initiate chemical reactions in normally inert gas mixtures [3]. The common thermal and catalytic techniques used for many years to eliminate NO_x and SO_x present in industrial or vehicle-generated fumes will not make it possible to respect the new emission limits which become more and more severe to protect the environment [4–6]. These effects can also have a direct impact on targeted applications such as electron beams particularly studied for the treatment of gaseous effluents polluted by nitrogen oxides, production of sulfur and/or ozone, medical applications and treament of surface [7,8]. The development of industrial and automotive activities in recent years has led to an increase in energy consumption, which has become increasingly important over the years [9,10]. This rapid growth in industrial and technological development has had a major impact on air quality, and has led to increased pollution most important As a result, the implementation of environmental standards on emissions compounds organic volatile as well as various oxides (NO_x, SO_x,...) has motivated the search for new ways of depollution [10]. Among the polluting species emitted in the atmosphere, it can be said that nitrogen monoxide NO and nitrogen dioxide NO_2 which are emissions mainly from combustion plants (i.e thermal power stations, solar heating...) and vehicles are the main pollutants in the atmosphere. The discharge of these effluents is now regulated and the standards are increasingly binding on industry and the automotive sector. These standards require the improvement of existing processing techniques or the development of new cleaner processes if they have reached their economic or technological limits [11–13].

The so-called conventional abatement techniques have successfully reduced harmful emissions. However, a new

technology based on non-thermal plasmas [14, 15] is used in many areas such as the control of gas pollution, production ozone, or surface treatment. Cold plasmas at atmospheric pressure exist in different forms. In this work, only plasmas generated by discharges point-to-plane crowns are modelled. This type of landfill is a very efficient active species. Pollution control by crown discharge requires two successive steps: the first, discharge phase which allows to generate by collisions between energetic electrons and gas molecules, active radicals such as O, N, OH, O_3...,the second, the post-discharge phase is where the formed radicals diffuse and react with the pollutants to destroy or transform them into new, less harmful species.

The numerical simulation that we will discuss in this paper concerns the spatial-temporal evolution of the density (radial and axial) of the species present in the gas mixture composed of 74 % N_2, 10 % O_2, 8 % H_2O and 8 % CO_2 (The choice of these species is related to their relative importance in polluted gases, especially oxides of azotes). The mixture is subjected to a point-to-plane of negative corona discharge with an inter-electrode distance equal to 20 mm (Fig. 1). These different species react to each other according to 80 chemical reactions. We consider the whole at room temperature and atmospheric pressure. The transfer of energy between the system electric and the gas mixture is modeled by the reduced electric field E/n. We have chosen the following three values 100, 200 and 300 Td (remember that 1Td=10^{-21} V.m^2)

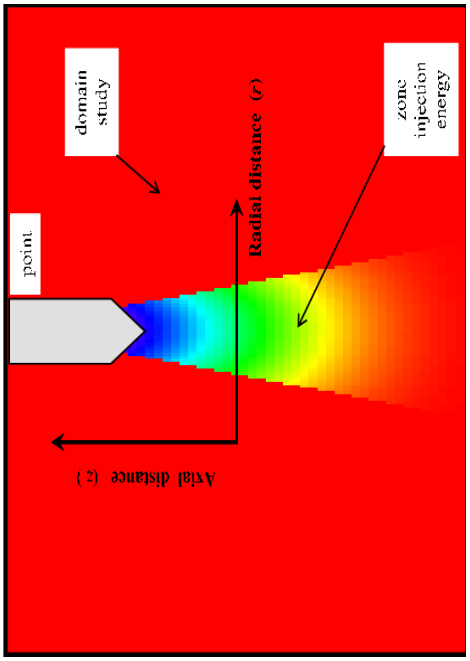

Figure 1. Schematic of a typical corona reactor geometry (pointed electrode and plane electrode).

II. BASIC FORMULAE

The mathematical model used in the present work consists of a system of equations that takes into account the variation of the density and the chemical kinetics of the environment, we adopt a developed order numerical code to resolve the transport equations. The algorithm is based on the time integration of the system of equations under consideration.

II.1. *Rate equation model*

In a volume-averaged approach, the state of the system is completely specified by the mass fractions of each species in the system, the temperature and the pressure. These properties change due to chemical reactions and the release of heat. Thus, we obtain the following conservation equations [16, 17].

Conservation of the overall mass m of the mixture, can be written as:

$$\frac{\partial(\rho\, V)}{\partial t} = \frac{\partial m}{\partial t} = 0 \tag{1}$$

where ρ is volume density (in kg m^{-3}), m denotes mass (in kg) and V is volume (in m^3).

Conservation of the species mass fraction ξ_i of species i, is defined by:

$$\frac{\partial \xi_i}{\partial t} - \frac{M_i\, \dot{\xi}_i}{\rho} = 0 \tag{2}$$

where ξ_i is mass fraction of the species i, $\dot{\xi}_i$ is rate of formation of the species i (in mol m^{-3} s^{-1}) and M_i is molar mass of the species i (in kg mol^{-1}).

Conservation of energy, can be written as:

$$\frac{\partial T}{\partial t} - \frac{1}{\rho\, C_p}\frac{\partial p}{\partial t} + \frac{1}{\rho\, C_p}\sum_i H_i\, M_i\, \dot{\xi}_i = 0 \tag{3}$$

where T is temperature, C_p molar heat capacity at the constant pressure (in J K^{-1} mol^{-1}), p is pressure and H_i is specific enthalpy of the species i (in J kg^{-1}).

To close this system of ordinary differential equations the ideal gas law:

$$p = \rho\, R\, T \sum_i \frac{\xi_i}{M_i} \tag{4}$$

where R is gas constant (in J K^{-1} mol^{-1}).

II.2. *Chemical kinetics*

The basic chemical kinetics used in the present paper, consist of a mathematical system of equations that takes into account the variation of the density and the chemical kinetics of the environment. The chemical kinetics equation systems can be described by an ordinary differential equation system obeying the following form [18].

$$\frac{d\, n_i}{d\, t} = \sum_{j=1}^{j_{\max}} F_{ij}, \qquad j \in [1, ..., j_{\max}] \tag{5}$$

where

$$F_{ij} = \varphi_{ij} - \chi_{ij} \tag{6}$$

n_i means the species densities vector, and F_{ij} mean the source term vector depending on the rate coefficient and

corresponding to the contributions from different processes. φ_{ij} and χ_{ij} represent respectively the gain and loss of species i due to the chemical reactions. The solution of such a system requires the knowledge of the initial concentrations.

However, the reactivity of the gas were taken into account to the source term F_{ij} (density conservation) Eq (5).

$$\varphi_{ij} = \sum_{\gamma} K_{\gamma}(T)(n_i\, n_j)_{\gamma} \tag{7}$$

and

$$\chi_{ij} = \sum_{\eta} K_{\eta}(T)(n_i\, n_j)_{\eta} \tag{8}$$

$K_{\gamma}(T)$ and $K_{\eta}(T)$ are the coefficients of the chemical reaction number γ or η, $(n_i\, n_j)$ means the product of densities of species i and j.

These coefficients satisfy Arrhenius formula [19]:

$$K_{\gamma}(T) = \kappa_1 \exp\left(\frac{\theta_{\gamma}}{T}\right) \tag{9}$$

and

$$K_{\eta}(T) = \kappa_2 \exp\left(\frac{\theta_{\eta}}{T}\right) \tag{10}$$

where κ_1 and κ_2 are the constant factors and θ_{γ} and θ_{η} are the activation energy of the chemical reaction.

The system of conservation equations are discretized by using a finite control volume with the approximation of a centred difference at the frontiers and solved by the F.C.T (Flux Corrected Transport) algorithm fully described by Refs. [20–22].

All the species considered in this simulation react with each other according to 80 chemical reactions which have been chosen in the literature and more precisely in the work on the chemical kinetics of industrial effluents [23–25]. It should be mentioned that all reactions taken into account and their reaction coefficients are shown in the Table 1.

III. RESULTS AND DISCUSSIONS

The results we will present in this section are shown below:

- Axial evolution of the density of nitrogen oxides NO, NO_2 and radicals N, O.
- Radial evolution of the density of nitrogen oxides NO and NO_2.

The spatial distribution of the density of two species that we have chosen NO and NO_2 for their contributions in this mixture, we present this distribution for different time in the ranges of 50-500 ns.

III.1. Evolution of nitrogen monoxide density NO

We present an axial and radial analysis of the evolution of the density of the NO molecule to better understand the reactivity of this species.

To analyse the axial evolution of the nitrogen monoxide density, we have shown in *at left* Fig. 2, changes in this species for three field values reduced electricity: (a): 100 Td, (b): 200 Td and (c): 300 Td. If we examine these graphs visually, we immediately notice a difference in the density of nitrogen monoxide for the three reduced electric fields. Indeed, Fig. 2(a), there is a variation in density between 10^6–10^8 m^{-3}, while for Fig. 2(b), the values records 10^7–10^9 m^{-3}, and for Fig. 2(c) we get asignificant variation between $10^{15} - 10^{17}$ m^{-3}. We can clearly see the influence of the transfer of energy ionised gas/neutral particle on the evolution of the density of nitrogen monoxide. It can also be noted in these Figs. (*at left* Fig. 2) that the more the intensity of the reduced electric field increases, the more the evolution of nitrogen monoxide in the inter-electrode space becomes significant. For example, in Fig. 2(a), we can see a significant increase in density between 50-250 ns along the axis of the discharge. Then, between ~ 300-500 ns the density begins to decrease with level of the point, while for the plane to the middle of the axis, it continues to increase. If we pass to Fig. 2(b), we notice the same phenomenon as before, except that in the cathode region the density becomes roughly equal to that of the point. For Fig. 2(c), the evolution of density is completely different from the previous two. In effect, from the beginning we notice a decrease in density throughout the axis of the with the appearance of three distinct zones: the plane zone, the central zone where the density is the lowest, and the point area with the highest density. We can therefore conclude that the energy injected into the gas mixture has a significant influence on the evolution of the nitrogen monoxide density over time.

To complete the previous analysis, we propose to see the behaviour of the molecule NO in the radial direction. For this we presented on the *at right* Fig. 2 density evolution for the same reduced electric field values. We notice on all the curves given on the two Fig. 2(a-b):

The convective movements that cause a slight depopulation of the axial area which varies over time.

The radial expansion towards the walls which decreases as one moves away from the discharge axis.

Regarding the Fig. 2(c) shows a very clear depopulation on the axis gradually over time and becomes very important from $t \simeq 400$ ns. Indeed, this decrease from $\sim 8 \times 10^{16}$ m^{-3} at $t = 50$ ns to $\sim 2 \times 10^{15}$ m^{-3} at $t = 450$ ns. This variation in density causes a blast wave to form at ~3 mm from the axis and reach its maximum at 15 mm from the axis. This depopulation on our axis the reduction of nitrogen monoxide, whereas for 100 and 200 Td we had a production of this species.

III.2. Evolution of the density of NO_2

Fig. 3 shows the time evolution of nitrogen monoxide density axial and radial for three values of the reduced electric field.

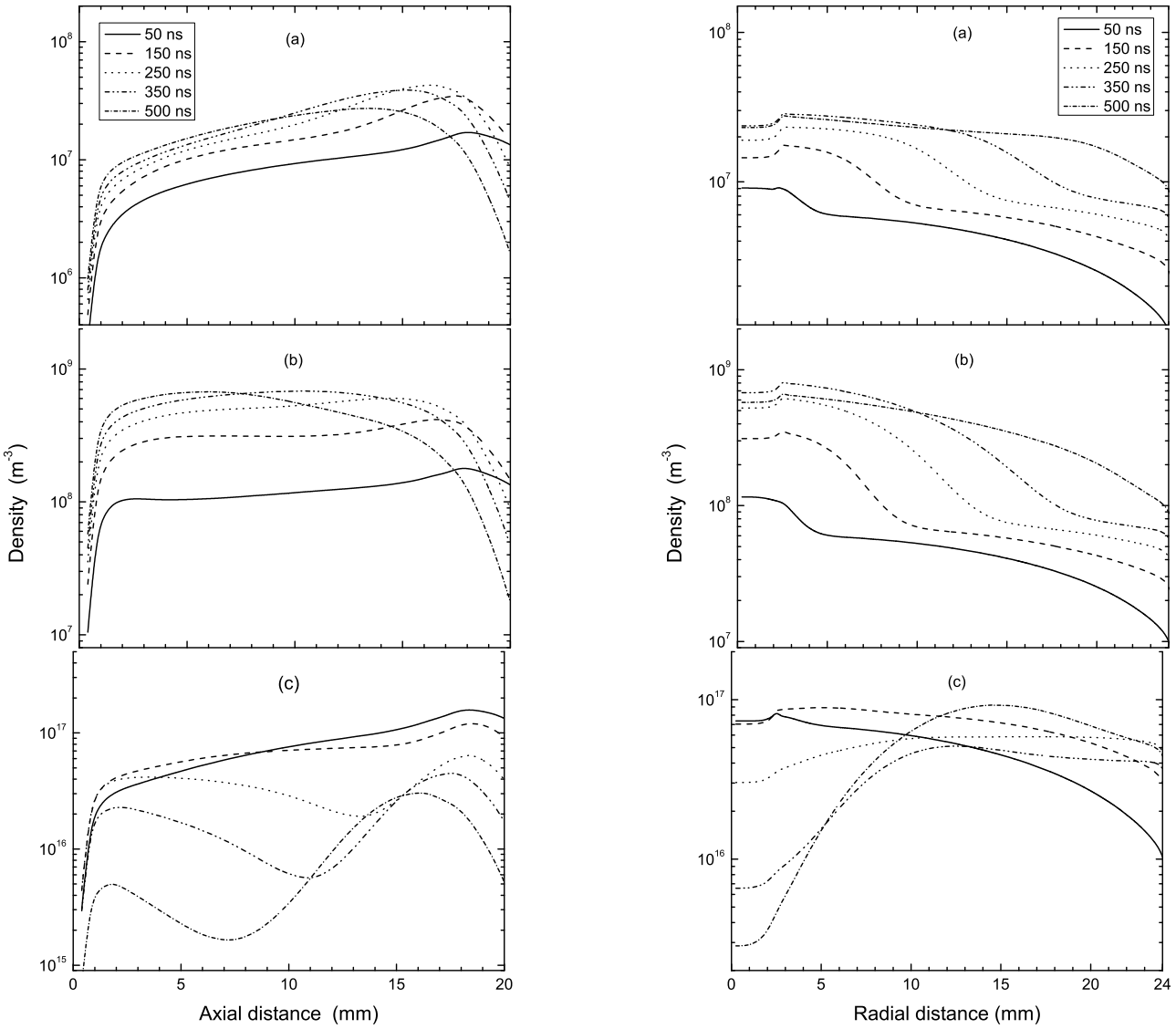

Figure 2. Evolution of the density of NO for a negative point discharge for three values of the reduced electric field, such as (a): 100 Td, (b): 200 Td and (c): 300 Td and for different times between 50 and 500 ns. At left axial evolution of NO; At right radial evolution of NO.

It is clearly seen that in *at left* Fig. 3(a,b) that there is a significant increase with the increase in time, this follows from the fact that there is a density more important depopulation in the inter-electrode space, whereas for Fig. 3(c) we have a decrease in density. For example, for 100 Td, there is a variation in density between $10^6 - 10^8$ m^{-3}, while for 200 Td, the values $10^7 - 10^9$ m^{-3}, and for 300 Td we get a variation between $10^{15} - 10^{16}$ m^{-3}. This is completely natural since nitrogen dioxide is created from nitric oxide by the following reaction:

$$O_3 + NO \rightarrow NO_2 + O_2$$

We also note on these curves (*at left* Fig. 3), that the more the intensity of the reduced electric field increases, the more the evolution of the density of nitrogen dioxide varies unevenly in the inter electrode space.

In Fig. 3(a) the density growth is seen along the discharge.

In Fig. 3(b), the density which was initially significant at the plane and minimal at the point becomes homogeneous in almost all space.

In Fig. 3(c), the density is completely different from the previous two since we have the appearance of three distinct zones: the plan, the center and the point, we also observe in Fig. 3(c) a density almost equal to the plane and point a density almost equal to the plane and at the point.

We can therefore conclude that part of the *at left* Fig. 3 is that the energy transfer between the plasma modeled by the reduced electric field and the NO_2 molecule which is created in the gas mixture, plays an important role in the evolution of density.

We now proceed to examine the behavior of the NO_2 molecule in the radial direction. In *at right* Fig. 3, we show the, the radial evolution of NO_2 for several times. We notice on all the curves that are given on the two Fig. 3(a-b):

The convective movements that cause a slight depopulation of the axial area which varies over time.

The radial expansion towards the walls that decreases as you move away the axis of the discharge.

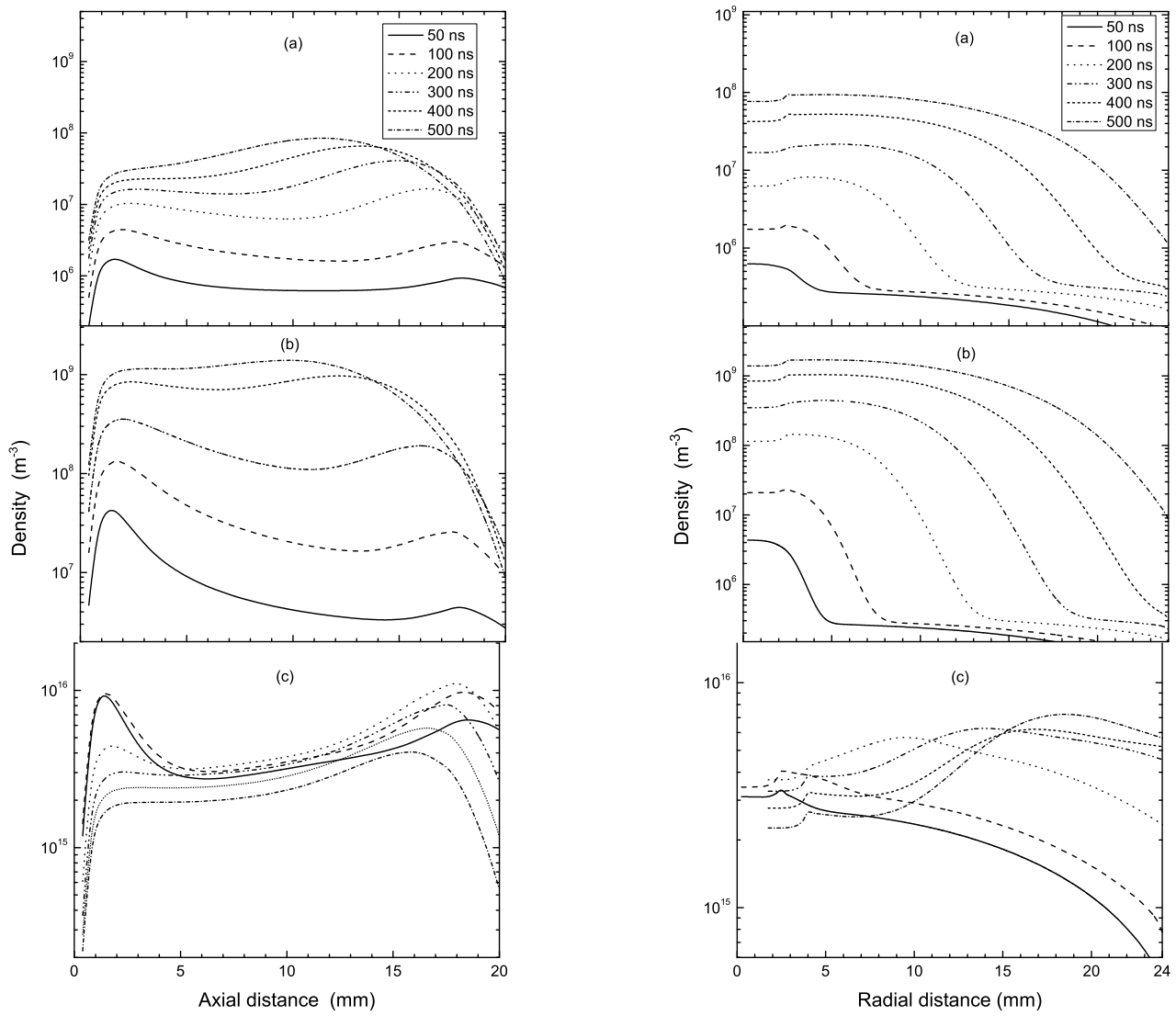

Figure 3. Evolution of the density of NO_2 for a negative point discharge for three values of the reduced electric field, such as (a): 100 Td, (b): 200 Td and (c): 300 Td and for different times between 50 and 500 ns. At left axial evolution of NO_2; At right radial evolution of NO_2.

In Fig. 3(c) shows a very clear depopulation on the axis gradually over time and becomes very important from $t \simeq 300$ ns. Indeed, this decay passes from $\sim 4\times10^{19}$ m^{-3} at $t = 50$ ns at the value $\sim 7\times10^{19}$ m^{-3} at $t = 500$ ns. This variation in density causes a blast wave to form at 3 mm from the axis and reach its maximum at 16 mm from the axis. This depopulation on our axis information on the reduction of nitrogen dioxide, whereas for 100 and 200 Td we had a production of this species.

III.3. Evolution of the density of N

In all the results presented previously in Figs. 2-3, we have presented as a function of evolution of the axial and radial density as a function of the inter-electrode space. In Figs. 4-5 we have represented the evolution of the density of nitrogen N for the three reduced electric fields as a function of the time, calculated for three different positions in inter-electrode space 6 mm, 12 mm and 18 mm. To better understand the evolution of nitrogen monoxide NO, because this last one is bound to nitrogen by reactions:

$$N + 2O \rightarrow NO + O$$

$$N + O + O_2 \rightarrow NO + O_2$$

$$N + O + N_2 \rightarrow NO + N_2$$

We observe, in the beginning from 50 ns to ~ 310 ns, a little rise of the density followed by a significant reduction especially for three values of the reduced electric fild. We note also that the N generation decreases with the increase of thereduced electric field. It is clear that the most significant differences the three position between in the vicinity of the point the heating starts to increase significantly.

III.4. Evolution of the density of O

We have shown in Fig. 6-7 our results for the evolution of the oxygen atom O for the three reduced electric fields as a

function of the time, shown for three selected positions: r = 6 mm, r = 12 mm and r = 18 mm. This radical also plays a role important in the conversion of nitrogen monoxide NO. It can be seen from Figs. 6-7 that the evolution, firstly depends on the inter-electrode space and secondly on the reduced electric field applied to the system. Indeed, heating is different for different chap selected.

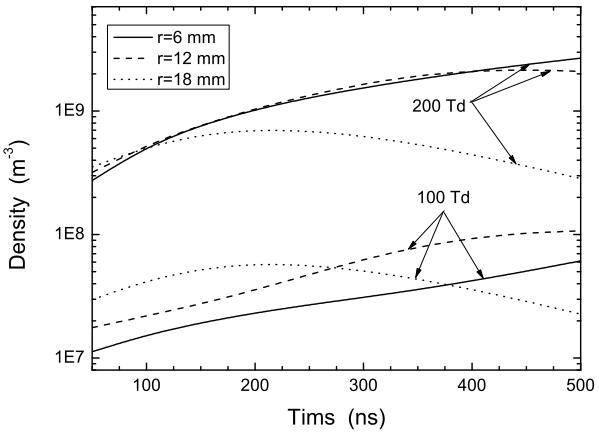

Figure 4. Evolution of the density of N for a negative point (with a 20 mm inter-electrode gap) discharge for two of the reduced electric field 100 Td and 200 Td, as a function of the time, shown for three selected positions: r = 6 mm, r = 12 mm and r = 18 mm.

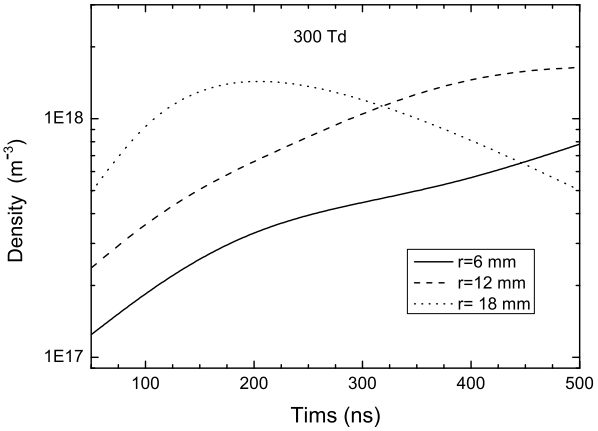

Figure 5. The same an in Fig. 4, but for other reduced electric field 300 Td.

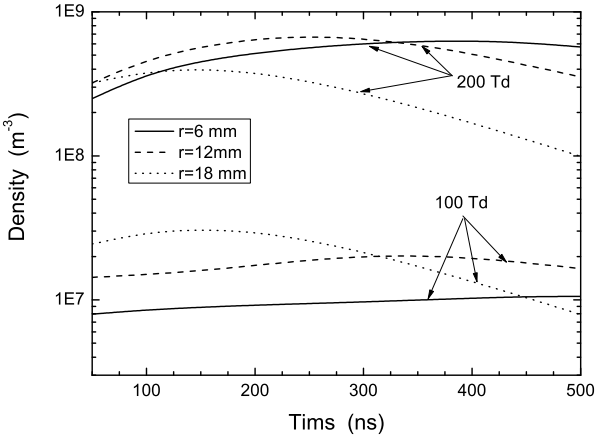

Figure 6. Evolution of the density of O for a negative point (with a 20 mm inter-electrode gap) discharge for two of the reduced electric field 100 Td and 200 Td, as a function of the time, shown for three selected positions: r = 6 mm, r = 12 mm and r = 18 mm.

From the results in Fig. 7 (i.e at 300 Td) it is clear that inclusion of the reduced electric field component can change considerably the density in the low-time range $t \simeq 50 - 200$ ns. At this range, for example, at r= 18 mm the evolution of density increases and reaches a maximum $\sim 5.52 \times 10^{17}$ m^{-3}, but it affects the reduced electric field of the density relatively moderately for $t \simeq 325$ ns. Now when r = 6 mm and 12 mm et $t \geq 330$ it increases rapidly the density, because of the heat flux which rise around the point region, the transfer of energy to neutral in our plasma is not spontaneous.

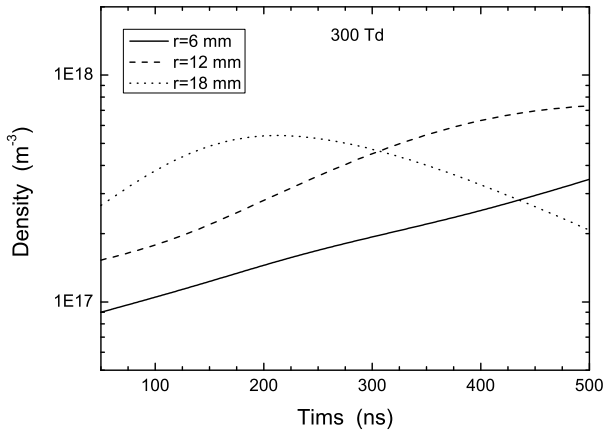

Figure 7. The same an in Fig. 6, but for other reduced electric field 300 Td.

IV. CONCLUSIONS

In this paper we have shown through a detailed analysis, the influence of energy transfer between the plasma (reduced electric field) and the neutral gas. This influence is observed on the NO and NO_2 species. The study is conducted for three values of the field reduced electric (100, 200 and 300 Td). Overall, the change in density caused by the diffusive movements of neutral particles, changes the spatial distribution of density.

The implemented equations are discretized by using a finite control volume with the approximation of a centred difference at the frontiers and solved by the F.C.T algorithm which allowed us to numerically simulate the spatio-temporal evolution of the density of two nitrogen oxides which are nitrogen monoxide NO and nitrogen dioxide NO_2 as well as the radicals N and O which are responsible for the creation of these two nitrogen oxides. The chosen gas mixture is a mixture of four species $N_2/O_2/H_2O/CO_2$ whose proportions are respectively 74 %, 10 %, 8 % and 8 %.

We can say that the ionized gas/neutral gas energy transfer, which we modeled by the reduced electric field, significantly influences the conversion of nitrogen oxides.

ACKNOWLEDGEMENTS

Dr A K FEROUANI gratefully acknowledges support from S.R.D.F.H.U, Algerian Ministry of Higher Education and Research (PRFU: B00L02UN130120190002).

Table 1. The main plasma reactions to generate the main radical to remove nitrogene oxides and their rate constants (in cm^3 $molecule^{-1}$ s^{-1}. $x[y]$ denotes $x \times 10^y$.

	Reaction	Rate Constants	Ref		Reaction	Rate Constants	Ref
R_1	$e^- + O_2 \rightarrow O + O + e^-$	15.0[-9]	[1]	R_{38}	$N + NO_2 \rightarrow N_2O + O$	0.15[-12]	[18]
R_2	$e^- + N_2 \rightarrow N + N + e^-$	2.00[-11]	[1]	R_{39}	$N + NO_2 \rightarrow 2NO$	0.15[-12]	[18]
R_3	$e^- + H_2O \rightarrow OH + H + e^-$	3.35[-10]	[1]	R_{40}	$N + N_2O \rightarrow N_2 + NO$	0.22[-1]	[18]
R_4	$e^- + CO_2 \rightarrow CO + O + e^-$	8.70[-11]	[1]	R_{41}	$N + O \rightarrow N + O$	0.07[-12]	[18]
R_5	$e^- + CO_2 \rightarrow CO + O^-$	3.60[-13]	[26]	R_{42}	$N + O_2 \rightarrow NO + O$	5.20[-12]	[26]
R_6	$N_2 + O_2 \rightarrow 2N + O_2$	0.11[-1]	[18]	R_{43}	$O + N_2 \rightarrow NO + N$	0.10[-5]	[18]
R_7	$N_2 + NO \rightarrow 2N + NO$	0.11[-1]	[18]	R_{44}	$O + O_2 + N_2 \rightarrow O_3 + N_2$	6.20[-34]	[26]
R_8	$N_2 + O \rightarrow 2N + O$	0.49[-1]	[18]	R_{45}	$O + 2O_2 \rightarrow O_3 + O_2$	0.30[-27]	[26]
R_9	$N_2 + N \rightarrow 3N$	0.49[-1]	[18]	R_{46}	$O + O_3 \rightarrow 2O_2$	0.80[-11]	[18]
R_{10}	$2N_2 \rightarrow 2N + N_2$	0.11[-1]	[18]	R_{47}	$O + N + O_2 \rightarrow NO + O_2$	$1.76[-31] \times T^{0.5}$	[27]
R_{11}	$O_2 + N_2 \rightarrow 2O + N_2$	0.33[-2]	[18]	R_{48}	$O + N + N_2 \rightarrow NO + N_2$	$1.76[-31] \times T^{0.5}$	[27]
R_{12}	$O_2 + NO \rightarrow 2O + NO$	0.33[-2]	[18]	R_{49}	$O + NO + O_2 \rightarrow NO_2 + O_2$	0.17[-27]	[18]
R_{13}	$O_2 + N \rightarrow 2O + N$	0.16[-1]	[18]	R_{50}	$O + NO + N_2 \rightarrow NO_2 + N_2$	0.17[-27]	[18]
R_{14}	$O_2 + O \rightarrow 3O$	0.16[-1]	[18]	R_{51}	$O + NO_2 \rightarrow NO + O_2$	0.52[-11]	[18]
R_{15}	$2O_2 \rightarrow 2O + O_2$	0.33[-2]	[18]	R_{52}	$O + NO_2 + O_2 \rightarrow NO_3 + O_2$	0.21[-26]	[18]
R_{16}	$N + O_2 \rightarrow NO + O$	8.90[-17]	[26]	R_{53}	$O + NO_2 + N_2 \rightarrow NO_3 + N_2$	0.21[-26]	[18]
R_{17}	$N + NO_2 \rightarrow N_2 + O + O$	0.91[-12]	[18]	R_{54}	$O + NO_3 \rightarrow O_2 + NO_2$	0.17[-10]	[26]
R_{18}	$N + NO_2 \rightarrow 2N_2$	0.23[-11]	[27]	R_{55}	$O + O + NO \rightarrow O_2 + NO$	0.19[-29]	[18]
R_{19}	$N + NO \rightarrow N_2 + O$	$1.05[-12] \times T^{0.5}$	[27]	R_{56}	$O + O + N \rightarrow O_2 + N$	0.95[-29]	[18]
R_{20}	$N + NO_2 \rightarrow N_2 + O_2$	0.70[-12]	[27]	R_{57}	$O + O + O \rightarrow O_2 + O$	0.95[-29]	[18]
R_{21}	$N + 2O \rightarrow NO + O$	0.66[-30]	[18]	R_{58}	$O + HNO_3 \rightarrow NO_3 + OH$	3.00[-15]	[26]
R_{22}	$N + O + NO \rightarrow NO + NO$	0.66[-30]	[18]	R_{59}	$2O + N_2 \rightarrow O_2 + N_2$	0.27[-30]	[26]
R_{23}	$N + NO_2 \rightarrow N_2 + O_2$	7.00[-13]	[27]	R_{60}	$2O + O_2 \rightarrow 2O_2$	0.27[-30]	[18]
R_{24}	$N + NO_2 \rightarrow N_2O + O$	0.24[-11]	[18]	R_{61}	$O + N_2 \rightarrow O + N_2$	0.18[-10]	[18]
R_{25}	$N + NO_2 \rightarrow 2NO$	0.60[-11]	[18]	R_{62}	$O + 2N_2 \rightarrow N_2O + N_2$	0.10[-34]	[18]
R_{26}	$N + CO_2 \rightarrow NO + CO$	$3.20[-13].\exp^{\frac{-1711}{T}}$	[18]	R_{63}	$O + N_2 + O_2 \rightarrow N_2O + O_2$	0.10[-34]	[18]
R_{27}	$2N + O_2 \rightarrow N_2 + O_2$	0.83[-33]	[18]	R_{64}	$O + O_2 \rightarrow O + O_2$	0.50[-11]	[18]
R_{28}	$2N + N_2 \rightarrow 2N_2$	0.83[-33]	[18]	R_{65}	$O + O_3 \rightarrow 2O + O_2$	0.12[-9]	[18]
R_{29}	$2N + NO \rightarrow N_2 + NO$	0.64[-25]	[18]	R_{66}	$O + O_3 \rightarrow 2O_2$	0.12[-9]	[18]
R_{30}	$2N + O \rightarrow N_2 + O$	0.27[-24]	[18]	R_{67}	$O + N_2O \rightarrow 2NO$	0.67[-10]	[18]
R_{31}	$3N \rightarrow N_2 + N$	0.27[-24]	[18]	R_{68}	$O + N_2O \rightarrow NO + O_2$	0.49[-10]	[18]
R_{32}	$2N + O \rightarrow NO + N$	0.66[-30]	[18]	R_{69}	$O + N_2O \rightarrow N_2 + O_2$	0.44[-10]	[18]
R_{33}	$OH + HNO_3 \rightarrow NO_3 + H_2O$	1.30[-13]	[26]	R_{70}	$O + NO_2 \rightarrow NO + O_2$	0.14[-9]	[18]
R_{34}	$OH + NO_2 \rightarrow HNO_3$	13.5[-11]	[18]	R_{71}	$O + NO \rightarrow N + O_2$	0.85[-10]	[18]
R_{35}	$N + N_2 \rightarrow N + N_2$	0.17[-13]	[18]	R_{72}	$NO + O \rightarrow O_2 + N$	0.13[-36]	[18]
R_{36}	$N + O_2 \rightarrow NO + O$	0.35[-12]	[18]	R_{73}	$O_3 + N \rightarrow NO + O_2$	0.10[-15]	[18]
R_{37}	$N + NO \rightarrow N_2 + O$	0.07[-10]	[18]	R_{74}	$O_3 + NO \rightarrow NO_2 + O_2$	0.18[-11]	[18]

V. REFERENCES

[1] K. Hatakeyama, S. Tanabe and Y. Hayashi et *al.*, J. Adv. Sci., **13**, 459 (2001).

[2] R. M. Balogh, I. Ionel and D. Stepan et *al.*, Termotehnica **2**, 32 (2011).

[3] J. S. Chang, Plasma Sources Sci. Technol. **17**, 045004 (2008)

[4] A. M. Pointu, A. Ricard and E. Odic et *al.*, Plasma Process. Polym. **5**, 559 (2008).

[5] M. Laroussi, A. Fridman and P. Favia et *al.*, Plasma Process. Polym. **7**, 193 (2010).

[6] A. K. Ferouani, M. Lemerini, L. Merad et *al.*, Plasma Sci. Technol. **17**, 469 (2015).

[7] J. Chen and J. H. Davidson, Plasma Chem. Plasma Process. **22**, 495 (2002).

[8] G. Fridman, G. Friedman, A., Shekhter et *al.*, Plasma Process. Polym. **5**, 503 (2008).

[9] M. Maulois, M. Ribière, and O. Eichwald et *al.*, Phys. Plasmas **23**, 043501 (2016).

[10] M. Bouzar, A. K. Ferouani and M. Lemerini et *al.*, High Temp. Mater. Process. **21**, 225 (2017).

[11] A. Mraihi, N. Merbahi and M. Yousfi et *al.*, Plasma Sources Sci. Technol. **20**, 065002 (2011).

[12] A. Abahazem, N. Merbahi, O. Ducasse et *al.*, IEEE Trans. Plasma Sci. **36**, 924 (2008).

[13] A. Abahazem, H. Guedah and N. Merbahi et *al.*, Mater. Today: Proceedings **2**, 4694 (2015).

[14] I. Orlandini and U. Riedel, Combust. Theory Model. **5**, 447 (2001).

[15] A. Haddouche amd M. Lemerini, Plasma Sci. Technol. **17**, 589 (2015).

[16] A. K. Ferouani, M. Lemerini and S. Belhour, Plasma Sci. Technol. **12**, 208 (2010).

[17] I. Orlandini and U. Riedel, J. Phys. D: Appl. Phys. **33**, 2467 (2000).

[18] O. Eichwald, N. A. Guntoro and M. Yousfi et *al.*, J. Phys. D: Appl. Phys. **35**, 439 (2002).

[19] A. Haddouche, " Etude électrique et physico chimique de la décharge couronne en vue de son application dans la réactivité des mélanges gazeux correspondants aux

effluents industriels". Tesis de doctorado, University Tlemcen-Algeria, 2015.
[20] J. P. Boris and D. L. Book, J. Comput. Phys. **11**, 38 (1973).
[21] J. P. Boris, F. F. Grinstein and E. S. Oran et *al.*, Fluid Dyn. Res. **10**, 199 (1992).
[22] D. Kuzmin, R. Löhner and S. Turek, Flux-corrected transport: principles, algorithms, and applications, (Springer Science, Business Media, 2012).
[23] R. Atkinson, D. L. Baulch and R. A. Cox et *al.*, J. Phys. Chem. Ref. Data **26**, 521 (1997).
[24] M. Yousfi, O.Eichwald and N. Merbahi et *al.*, Plasma Sources Sci. Technol. **21**, 045003 (2012).
[25] M. Bafoil, A. Jemmat and Y. Martinez et *al.*, PloS one **13**, 1 (2018).
[26] O. Eichwald, M. Yousfi, A. Hennad et *al.*, J. Appl. Phys. **82**, 4781 (1997).
[27] I. A. Kossyi, A. YuKostinsky, A. A. Matveyev et *al.*, Plasma Sources Sci. Technol. **1** 207 (1992).